Annals of Nuclear Medicine Vol. 12, No. 3, 127–132, 1998

Use of automated image registration to generate mean brain SPECT image of Alzheimer's patients

Muhammad Babar IMRAN,* Ryuta KAWASHIMA,* Shuichi AWATA,** Kazunori SATO,* Shigeo KINOMURA,* Hiroshi ITO,* Shuichi ONO,* Seiro YOSHIOKA,* Mitsumoto SATO** and Hiroshi FUKUDA*

*Department of Nuclear Medicine and Radiology, Institute of Development, Aging and Cancer, Tohoku University
**Department of Psychiatry, Tohoku University Hospital

The purpose of this study was to compute and compare the group mean HMPAO brain SPECT images of patients with senile dementia of Alzheimer's type (SDAT) and age matched control subjects after transformation of the individual images to a standard size and shape. *Methods:* Ten patients with Alzheimer's disease (age 71.6 ± 5.0 yr) and ten age matched normal subjects (age 71.0 ± 6.1 yr) participated in this study. Tc-99m HMPAO brain SPECT and X-ray CT scans were acquired for each subject. SPECT images were normalized to an average activity of 100 counts/pixel. Individual brain images were transformed to a standard size and shape with the help of Automated Image Registration (AIR). Realigned brain SPECT images of both groups were used to generate mean and standard deviation images by arithmetic operations on voxel based numerical values. Mean images of both groups were compared by applying the unpaired t-test on a voxel by voxel basis to generate three dimensional T-maps. X-ray CT images of individual subjects were evaluated by means of a computer program for brain atrophy. *Results:* A significant decrease in relative radioisotope (RI) uptake was present in the bilateral superior and inferior parietal lobules ($p < 0.05$), bilateral inferior temporal gyri, and the bilateral superior and middle frontal gyri ($p < 0.001$). The mean brain atrophy indices for patients and normal subjects were 0.853 ± 0.042 and 0.933 ± 0.017 respectively, the difference being statistically significant ($p < 0.001$). *Conclusion:* The use of a brain image standardization procedure increases the accuracy of voxel based group comparisons. Thus, intersubject averaging enhances the capacity for detection of abnormalities in functional brain images by minimizing the influence of individual variation.

Key words: Alzheimer's dementia, Tc-99m HMPAO SPECT, image registration

INTRODUCTION

ALZHEIMER'S DISEASE is a primary neuronal disorder causing progressive loss of neurons and neuronal activity. Secondary to this change, there is a reduction in regional cerebral blood flow (rCBF),[1] so that striking abnormalities in rCBF have been detected in Alzheimer's patients by a variety of techniques including PET[2] and perfusion SPECT.[3–5] Although the predominant rCBF pattern observed with high posterior probability is one of bilateral parieto temporal abnormality,[6] other patterns of rCBF deficits have also been reported for patients suffering from senile dementia of Alzheimer type (SDAT).[7,8] However subjective evaluation employed in these cases for comparison with controls meant that the sensitivity of the rating procedures was limited.

Image averaging improves the signal to noise ratio and takes into accounts individual variance, making the evaluation more objective.[9,10] While such averaging procedures enhance the confidence of findings, they require transformation of the individual images into a specific/standard size and shape. The availability of various analyses,

Received October 29, 1997, revision accepted March 2, 1998.

For reprint contact: Muhammad Babar Imran, MBBS. MS (Nuclear Medicine), Department of Nuclear Medicine and Radiology, Division of Brain, Sciences, Institute of Development, Aging and Cancer, Tohoku University, 4–1 Seiryo machi, Aoba-ku, Sendai 980–8575, JAPAN.

including arithmetical and statistical calculations on a pixel by pixel basis means that a high degree of precision can be achieved.[11] Thus any deviation from the normal pattern can be recognized and mapped out on the standard template.

Recently several studies have been performed with the principle of standardization.[12-14] Group mean images of normal control subjects and patients' images have been generated and compared to map the significant differences.[15] Pixel by pixel comparisons of different images are more accurate and reproducible than region of interest (ROI) analyses. Voxel based comparison can detect small changes that may not be distinguished by other types of analyses because of their subjectivity or partial volume effects.

Approaches to alignment/standardization of tomographic images include manual superimposition and derivation of transformation matrices between images based on their edge location in combination with other fiducial markers,[16] as well as methods based on area related parameters and image correlation.[17,18] These vary in their accuracy depending on the amount of information used in computing the transformation matrices. AIR is a program, recently developed by Woods et al.,[19-21] which realigns and registers any brain image with respect to another specified reference image. Registration parameters are computed only taking into account voxel based functional data. The cost function based on standard deviation of pixel by pixel ratios (other optional cost functions are also available), is minimized to optimize the transformation process. Since the program is non interactive and fully automated, the results of AIR are consistent and reproducible. It has been applied for various types of registrations, including intersubject SPECT images.[19,20,22-26]

In this study we used AIR to standardize the size and shape of individual brain SPECT images of Alzheimer patients and age matched normal subjects. Arithmetic calculations were performed on voxel values of individual images to generate three dimensional group mean images for further analyses.

MATERIALS AND METHODS

A total of 10 patients with Alzheimer's disease (age 71.6 ± 5.0 yr) and 10 age matched normal subjects (age 71.0 ± 6.1 yr) participated in the study. Written informed consent was obtained in all cases according to the declaration of human rights of Helsinki 1975. All the subjects were right handed as assessed by the H.N. handedness inventory. None of the control subjects had any previous signs or symptoms of any disease that could effect CBF studies, and demonstrated normal X-ray CT scans taken immediately after SPECT measurements. All of the patients had been in follow up for at least one year after clinical diagnosis of probable SDAT according to the Diagnostic and Statistical Manual of Mental Disorders (DSM-IV) and National Institute for Neurological & Communicative Disorders & Stroke/Alzheimer's Disease & Related Disorders Association (NINCDS-ADRDA). Patients were examined according to mini mental state (MMS) and clinical dementia rating (CDR) scales. CDR was rated 1 for all the patients and the MMS score ranged from 16 to 22 in these patients, confirming early and mild stage SDAT. SPECT studies were performed on patients before starting any medication, but their scans were included in the study after completion of a one year follow up, to make sure that all the subjects had SDAT.

SPECT

Each SPECT scan was performed 10 minutes after an intravenous bolus injection of Tc-99m HMPAO (1036–1054 MBq) with the subject lying supine with eyes closed during the injection and acquisition periods. A SPECT scanner (SPECT-2000H, Hitachi Medico Corp, Tokyo, Japan),[27] incorporating a four head rotating camera with an in-plane and axial resolution of 8 mm full width at half maximum (FWHM) fitted with low energy—high resolution collimators, was used for all measurements. Image reconstruction was performed by filtered back projection with a Butterworth filter (dimension 12, cut off 0.25 cycle/pixel). Attenuation correction was made numerically by assuming the object shape to be an ellipse for each slice and the attenuation coefficient to be uniform (0.1/cm). Correction for scatter photons was not performed. Image slices were set up parallel to the cantho-meatal (CM) line and obtained at 8 mm intervals through the entire brain. After SPECT measurements, X-ray CT scans were obtained with the same CM line as applied for SPECT in all subjects. All reconstructed images were transferred to a UNIX Work Station for further analysis.

Mean image generation

SPECT images were globally normalized by averaging the whole brain radioactivity to 100 counts per pixel. After this normalization, all SPECT images were registered with respect to a standard image to make target images similar in size and shape by AIR, using linear and non-linear parameters. The option of unidirectional fitting was selected during affine model fitting. Sinc interpolation was used to avoid post reconstruction resampling artifacts. Smoothing of images was done with a Gaussian filter with isotropic dimensions of 10 mm. The mean SPECT HMPAO image of 18 normal subjects obtained in another study[12] in this department with HBA system[28] was taken as a standard. Therefore, after standardization by AIR, the brain image of each subject was transformed into the same size and shape as the standard brain of the HBA system. Then mean and standard deviation images were calculated on a voxel by voxel basis for patients and control subjects.

The mean HMPAO brain SPECT image of the patients was statistically compared with that for the control group,

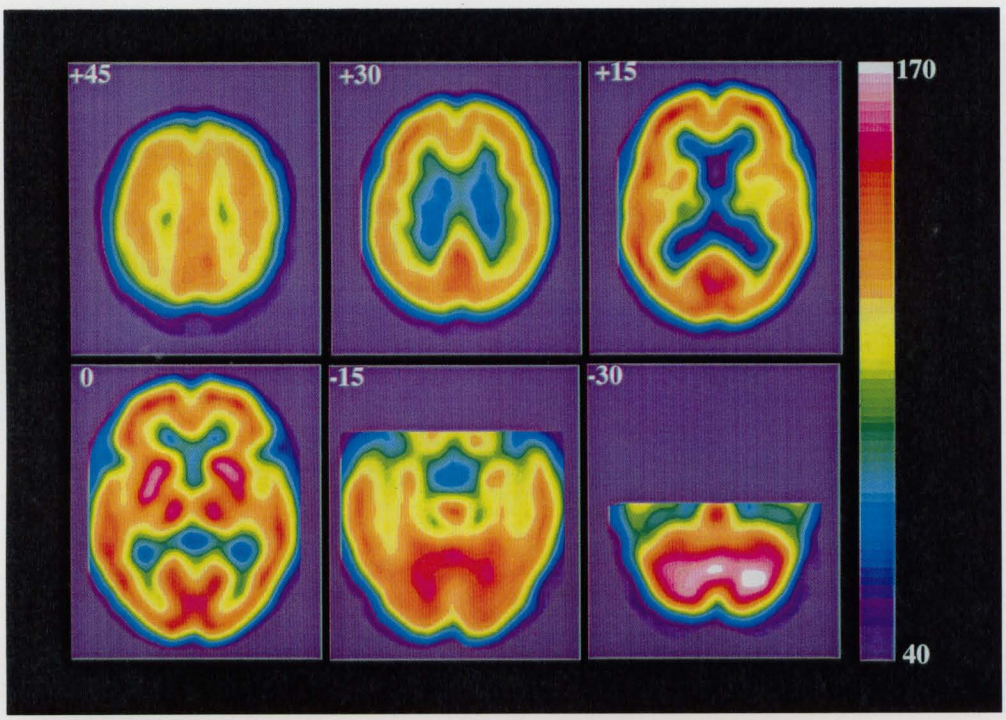

a

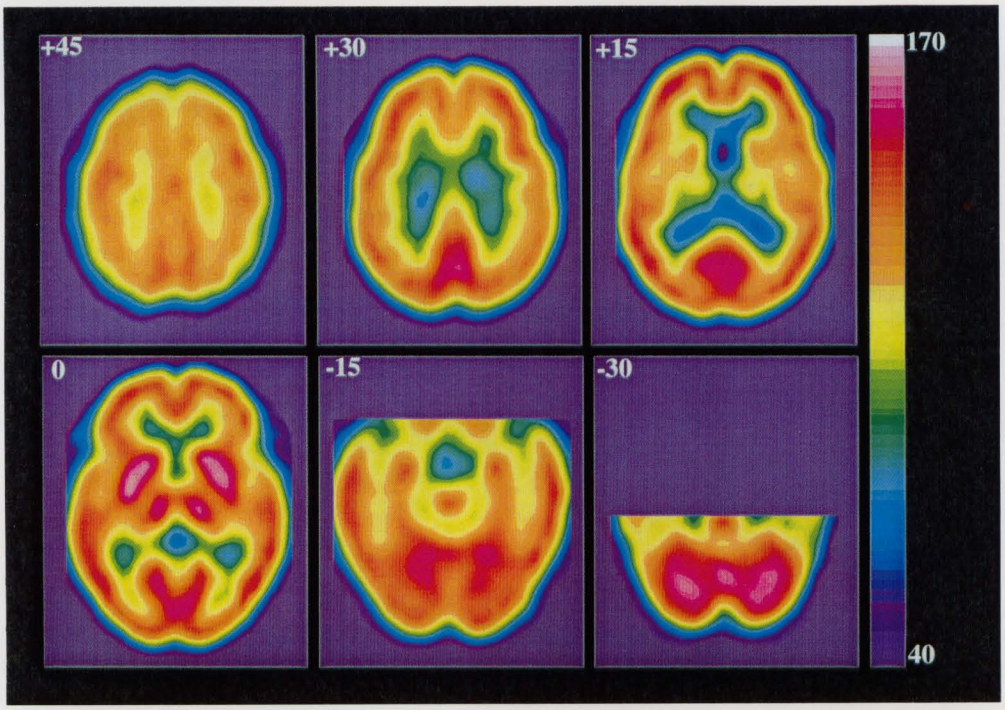

b

Fig. 1 Group mean Tc-99m HMPAO SPECT images of SDAT patients (a) and normal subjects (b). The mean global value is 100 counts/pixel. Horizontal slices are with reference to the Telairach grid. The anterior represents the top of the image and subject's right is on the left.

voxel by voxel. The two sample t-test was applied and resulting t values were displayed as color codes on the corresponding pixels to generate three dimensional T-maps after cluster analysis. Values over 2.1 were taken as statistically significant, corresponding to a level of $p < 0.05$.

X-ray CT scans of all the subjects were evaluated by radiologists for any abnormality and a Brain Atrophy

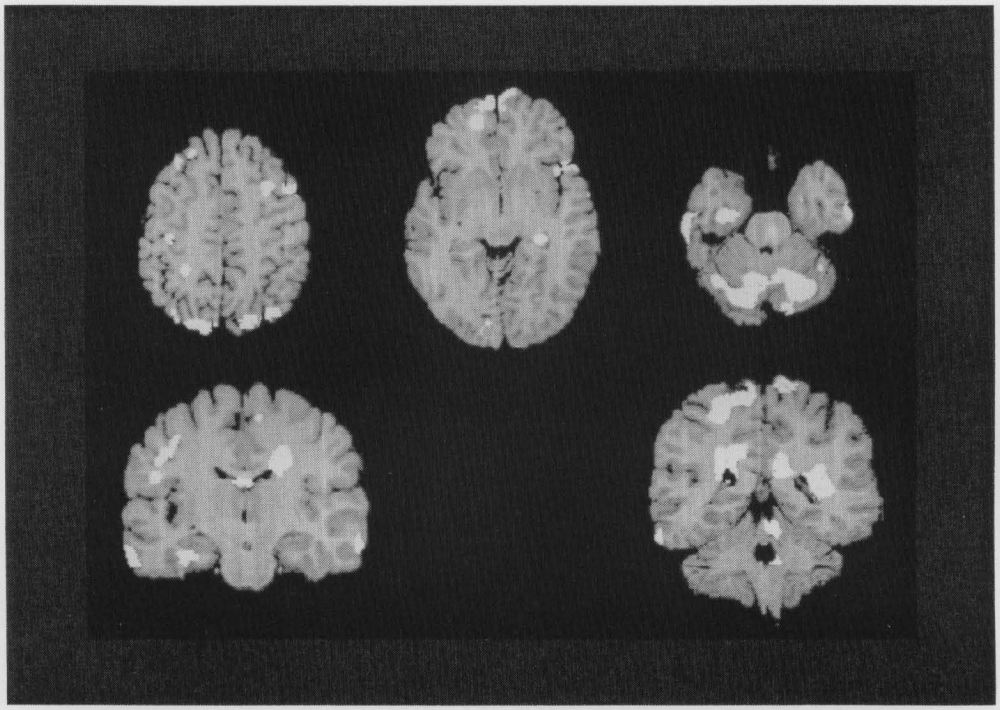

Fig. 2 T-map showing two sample 't' values (mean image of normal subjects – mean image of SDAT patients) displayed on corresponding pixels of the brain image superimposed on MRI. The threshold setting is at 2.1 corresponding to a significance level of $p < 0.05$.

Index (BAI) was calculated for each subject with a computer program.[29] Brain tissue, cranial bone and CSF space were specified with their CT numbers at CT sections 50 mm to 90 mm above the CM line with an interslice interval of 10 mm. The cut-off level of CT numbers for the brain from CSF was 22 and that for bone from CSF was 200. The BAI was calculated as:

$$\text{BAI} = \frac{\text{Volume of CSF Space}}{\text{Volume of Cranial Cavity}} \times 100$$

RESULTS

Figure 1 (a, b) shows mean rCBF images of patients and age matched control subjects. Mean images of patients with SDAT show bilateral parieto temporal deficits. In addition to this, frontal regions also show lower uptake of radioactivity. Ventricular/periventricular regions, the distance between caudate nuclei (slice at 0 level) and lateral sulci are wider in the patients' group. These findings are consistent with morphological data of X-CT scans. Figure 2 shows a T-map of significant differences in the bilateral superior and inferior parietal lobules, bilateral inferior temporal gyri, bilateral superior frontal gyri, and cerebellum and white matter ($p < 0.05$).

Brain atrophy indices calculated with the computer program significantly differed between the two groups ($p < 0.001$), the mean values being 0.853 ± 0.042 and 0.933 ± 0.017 for patients and controls, respectively.

DISCUSSION

Dementia is a common problem of old age and Alzheimer's disease is by far the most prevalent type, accounting for about two thirds of all the cases.[30] SPECT CBF imaging is an important tool for diagnostic work up of SDAT patients. The present prospective study, aimed at the evaluation of rCBF abnormalities in group mean images of Alzheimer's patients revealed decreased metabolism in the frontal, parietal and temporal lobes, but the primary cortical areas and subcortical regions were unaltered.

Differences in the RI uptake value in almost all the cortical regions were apparent in mean rCBF images of patients and control subjects (Fig. 1a, b), but statistical significance was limited to severely degraded areas apparent on the T-map (Fig. 2). Metabolic disturbances of cerebral regions noted in SDAT patients were statistically significant only when the disruption was massive. This might be related to the fact that these measures have a smaller variance than the absolute metabolic rates (10% vs. 20–30%).[31]

Changes in functional coupling between various regions of the brain could not be explained by simple geriatric change because of its lack in controls. The relatively increased uptake of RI in mean images of the patients' group in white matter and cerebellum reflects the global normalization (taking whole brain activity as a reference). As assessed in most clinical studies, we here

mainly considered changes in relative CBF. Since medication may effect CBF images through metabolic alterations,[32-35] we performed our studies before starting any medication, to avoid this problem.

Although brain image standardization and averaging facilitate pixel by pixel comparisons, theoretically error could arise from the original rCBF values. The standard brain image used in our study was the mean of HMPAO images for healthy volunteers with an average age of 51 (range 34–63 years). The average age of the target subjects, in contrast, was around 70 years, but, because both groups are treated equally, this effect may have been minimized if not canceled out altogether. The interpolation artifacts during post-reconstruction resampling were minimized by using sinc interpolation. Other factors which may lead to erroneous results could be differences in partial volume effects during discrete sampling of the signal and systematic biases during unidirectional reorientation of images. These factors are more deleterious for ROI type of analyses than voxel based comparisons. Considering these factors we limit our analysis to T-maps. Even then caution should be taken and individual results should be assessed carefully.

Relatively advanced atrophy observed in patients appears due to disease rather than simple aging processes. Effects of atrophy itself on rCBF SPECT images were not corrected because atrophy contains information related to the disease process. Moreover, we believe that comparison with age matched normal subjects cancels out any atrophy related to physiological aging. The remaining part of atrophy is merely due to disease, which should be evaluated as a part of the results. In one of our previous reports, we successfully registered SPECT images after introduction of artificial cold defects (equal to 20 m*l* volume) with the help of AIR.[25] Extrapolation to the clinical environment suggests that advanced atrophy in patients does not yield or propagate any error during registration of SPECT rCBF images by AIR.

Most studies assessing the accuracy of SPECT in SDAT have been retrospective with patient selection based on the diagnosis established at the time of scintigraphic evaluation. Prospective and consecutive studies, while difficult to perform because of the long follow up, are more accurate guides for clinical practice.[36] We therefore coupled our image analysis of consecutive cases with a clinical follow up of sufficient duration to reduce diagnostic uncertainty. As a result, the number of the patients that could be definitely classified as having SDAT was only 46% (10/22) of the total patient population at the commencement. To our knowledge this is the first HMPAO SPECT study performed on strictly screened patients and aimed at the preparation of a mean image for Alzheimer's patients after registration of individual images by AIR. Effective comparison of group mean images of patients with that of age matched normal subjects thereby proved possible and the data generated in this prospective study should be useful as a reference for future projects.

CONCLUSIONS

Use of the standardization procedure enhances the confidence of characteristic findings. It also facilitates voxel based comparisons (intersubject/intrasubject) allowing increased sensitivity and precision. Thus this pixel by pixel approach can detect small changes that may be overlooked by other types of analyses because of their subjectivity or partial volume effects.

ACKNOWLEDGMENTS

We are greatly indebted to the staff of the Institute of Development, Aging and Cancer, Tohoku University, and in particular Mr. Tachio Sato, for his technical help during acquisition of the SPECT images. This study was supported by a Research Grant for Health and Sciences, Research Grant for Aging and Health, from The Telecommunication Advancement Foundation, Japan and a Grant in aid for Scientific Research and Priority Areas from The Ministry of Education, Science, Sports and Culture, Japan.

REFERENCES

1. Legg NJ, Frackowiak RSJ. Positron emission tomography in dementia. *Interdiscipl Topics Geront* 20: 67–70, 1985.
2. Frackowiak RSJ, Pozzilli C, Legg NJ, et al. Regional cerebral oxygen supply and utilization in dementia. A clinical and physiological study with oxygen 15 and positron tomography. *Brain* 104: 753–778, 1981.
3. Cohen MB, Graham LS, Lake R, et al. Diagnosis of Alzheimer's disease and multiple infarct dementia by tomographic imaging of iodine 123-IMP. *J Nucl Med* 27: 769–774, 1986.
4. Sharp P, Gemmell H, Cherryman G, Besson J, Crawford J, Smith F. Application of iodine 123-labeled IMP imaging to the study of dementia. *J Nucl Med* 27: 761–768, 1986.
5. Smith FW, Besson JAO, Gemmell HG, Sharp PF. The use of technetium-99m HMPAO in the assessment of patients with dementia and other neuropsychiatric conditions. *J Cereb Blood Flow Metab* 8: S116–S122, 1988.
6. Holman BL, Johnson KA, Gerada B, Carvalho PA, Satlin A. The scintigraphic appearance of Alzheimer's disease: A prospective study using Tc-99m HMPAO SPECT. *J Nucl Med* 33: 181–185, 1992.
7. Costa DC, Ell PJ, Burn A, Philpot M, Levy R. CBF tomograms with Tc-99m HMPAO in patients with dementia and Parkinson's disease. *J Cereb Blood Flow Metab* 8: S109–S115, 1988.
8. Neary D. Snowden JS, Northn B, Goulding P. Dementia of frontal lobe type. *J Neurol Neurosurg Psychiatry* 51: 353–361, 1988.
9. Fox PT, Mintun MA, Reiman EM, Raichle ME. Enhanced detection of focal brain responses using intersubject averaging and change distribution analysis of subtracted PET images. *J Cereb Blood Flow Metab* 8: 642–653, 1988.

10. McCready R, A'Hern R. A more rational basis for determining the activities used for radionuclide imaging? *Eur J Nucl Med* 24: 109–110, 1997.
11. Eberl S, Kanno I, Fulton RR, Ryan A, Hutton BF, Fulham MJ. Automated interstudy image registration technique for SPECT and PET. *J Nucl Med* 37: 137–145, 1996.
12. Koyama M, Kawashima R, Ito H, et al. Normal cerebral perfusion of Tc-99m HMPAO brain SPECT—Evaluation by an Anatomical Standardization Technique—. *KAKU IGAKU (Jpn J Nucl Med)* 32: 967–977, 1995.
13. Koyama M, Kawashima R, Ito H, Ono S, Sato K, Goto R, et al. SPECT images with Tc-99m HMPAO and Tc-99m ECD in normal subjects. *J Nucl Med* 38: 587–592, 1997.
14. Ono S, Kawashima R, Ito H, Koyama M, Goto R, Inoue K, et al. Regional distribution of muscarinic cholinergic receptor in the human brain studied with C-11 Benztropine and PET using an anatomical standardization technique. *KAKU IGAKU (Jpn J Nucl Med)* 33: 721–727, 1996.
15. Ito H, Kawashima R, Awata S, et al. Hypoperfusion in the limbic system and prefrontal cortex in depression: SPECT with anatomic standardization technique. *J Nucl Med* 37: 410–414, 1996.
16. Evans A, Beil C, Marret C, Thompson C, Hakim A. Anatomical functional correlation using an adjustable MRI based ROI atlas with positron emission tomography. *J Cereb Blood Flow Metab* 8: 513–530, 1988.
17. Alpert N, Bradshaw J, Senda M, Correia J. The principal axis transformation: a method for image registration. *J Nucl Med* 30: 776, 1989.
18. Junck L, Moen JG, Hutchins GD, Brown MB, Kuhl DE. Correlation methods for centering, rotating, and alignment of functional brain images. *J Nucl Med* 31: 1220–1226, 1990.
19. Woods RP, Grafton ST, Holmes CJ, Cherry SR, Mazziotta JC. Automated image registration: I. General method and intrasubject, intramodality validation. *J Comput Assist Tomogr* 22: 141–154, 1998.
20. Woods RP, Grafton ST, Watson JDG, Sicotte, Mazziotta JC. Automated image registration: II. Intersubject validation of linear and nonlinear models. *J Comput Assist Tomogr* 22: 155–165, 1998.
21. Woods RP, Mazziotta JC, Cherry SR. Automated image registration. In: *Quantificaiton of Brain Function.* Tracer kinetics and image analysis in brain PET. Uemura K, et al., eds. Elsevier Science Publisher, pp. 391–398, 1993.
22. Strother SC, Anderson JR, Xu SI, Liow JS, Bonar DC, Rottenberg DA. Quantitative comparisons of image registration techinques based on high resolution MRI of the brain. *J Comput Assist Tomogr* 18: 954–962, 1994.
23. Black KJ, Videen TO, Perlmutter JS. A metric for testing the accuracy of cross modality image registration: Validation and application. *J Comput Assist Tomogr* 20: 855–861, 1996.
24. Imran MB, Kawashima R, Sato K, Kinomura S, Inoue K, Ono S, et al. Evaluation of accuracy in inter subject transformation of brain SPECT images using automated image registration (AIR). *Ann Nucl Med* 10 (Suppl): S222, 1996. (abstract)
25. Kinomura S, Kawashima R, Sato K, Imran MB, Yoshioka S, Ono S. Intersubject transformation of Brain SPECT by automated image registration (AIR)—Effects of defects in the target image—. *Ann Nucl Med* 10 (Suppl): S222, 1996. (abstract)
26. Imran MB, Kawashima R, Sato K, Kinomura S, et al. Mean rCBF images of normal subjects using Tc-99m HMPAO by automated image registration (AIR). *J Nucl Med* 39: 203–207, 1998.
27. Kimura K, Hashikawa K, Wtani H, et al. A new apparatus for brain imaging: four head rotating gamma single photon emission computed tomography. *J Nucl Med* 31: 603–609, 1990.
28. Roland PE, Graufelds CJ, Wahlin J, et al. Human brain atlas: For high resolution functional and anatomical mapping. *Hum Brain Mapp* 1: 173–184, 1994.
29. Takeda S, Matsuzawa T. Brain atrophy during aging: A quantitative study using computed tomography. *J Am Geriatr Soc* 32: 520, 1984.
30. Chui HC. Dementia, a review emphasizing clinicopathological correlation and brain behavior relationships. *Arch Neurol* 46: 806–814, 1989.
31. Haxby JV. Letter to the editor. *J Cerebr Blood Flow Metab* 6: 125–126, 1986.
32. Kobari M, Fukuuchi Y, Shinohara T, Obara K, Nogawa S. Levodopa induced local cerebral blood flow changes in Parkinson's disease and related disorders. *J Neurol Sci* 128: 212–218, 1995.
33. Heiss WD, Hebold H, Klinkhammer P. Effect of piracetam on cerebral glucose metabolism in Alzheimer's diesease as measured by positron emission tomography. *J Cereb Blood Flow Metab* 8: 613–617, 1988.
34. Geaney DP, Soer N, Shepstone BJ, Cowen PJ. Effect of central cholinergic stimulation on regional cerebral blood flow in Alzheimer disease. *Lancet* 335: 1484–1487, 1990.
35. Harkins SW, Taylor JR, Mattay US. Response to tacrine in patients with dementia to Alzheimer's type: cerebral perfusion change related to change in mental status. *Int J Neurosc* 84: 149–156, 1996.
36. Launes J, Sulkara R, Erkijuntti T, et al. Tc-99m HMPAO SPECT in suspected dementia. *Nucl Med Commun* 12: 757–765, 1991.